

Characteristics of layered polar mesosphere summer echoes occurrence ratio of polar mesosphere summer echoes-observed by EISCAT VHF 224MHz Radar

5 Shucan Ge¹, Hailong Li¹, Tong Xu², Mengyan Zhu², Maoyan Wang¹, Lin Meng¹, Safi Ullah¹, Abdur Rauf¹

¹School of Electronic Science and Engineering, University of Electronic Science and Technology of China, 610054, Chengdu, China

10 ²National Key Laboratory of Electromagnetic Environment, China Research Institute of Radiowave Propagation, 266107, Qingdao, China

Correspondence to: Hailong Li (hailong703@163.com)

Abstract. Polar Mesosphere Summer Echoes (PMSE) are strong radar echoes observed in polar mesopause during local summer. ~~Observations~~Measurements of layered PMSE ~~observed-carried out by~~ the European Incoherent Scatter Scientific Association Very high frequency (EISCAT VHF) radar ~~from 2004 to 2015~~during 2004-2015 in the latest solar cycle; ~~can be~~ used to study the variations of PMSE occurrence ratio (OR). ~~Different seasonal behavior of PMSE is found by analyzing the seasonal variation of PMSE mono-, double- and tri-layer OR.~~The seasonal variation of PMSE mono-, double- and tri-layer ~~occurrence ratio was analyzed, and there is different seasonal behavior.~~ A method was ~~given-used~~ to calculate the PMSE mono-, double- and tri-layer ~~occurrence ratio~~OR under different electron density threshold ~~conditions~~. In addition, ~~a method to analyze~~ the correlation ~~between-of layered~~ PMSE ~~layered occurrence ratios~~OR ~~and with~~ solar 10.7 cm flux index ($F_{10.7}$), ~~and the correlation between PMSE layered occurrence ratios~~ and geomagnetic K index ~~were-is proposed~~analyzed respectively in this study. And base on it, the correlation of layered PMSE OR with solar and geomagnetic activities is not expected to affect by discontinuous PMSE. It ~~can be obtained~~is found that PMSE mono-, double- and tri-layer OR are positively correlated with the K index. The correlation ~~coefficient-of-between~~ PMSE mono- and double-layer OR ~~and with~~ $F_{10.7}$ is weak, ~~and-whereas~~ the PMSE tri-layer OR ~~has-shows~~ a negative correlation with $F_{10.7}$.

Keywords: Polar Mesosphere Summer Echoes; ~~European Incoherent Scatter Scientific Association Very high frequency Radar~~EISCAT VHF radar; solar 10.7 cm flux index ($F_{10.7}$) ; geomagnetic K index

设置了格式: 上标

设置了格式: 非上标/下标

设置了格式: 下标

设置了格式: 下标

设置了格式: 下标

设置了格式: 下标

1 Introduction

The ionosphere is an important part of near the ~~earth~~-Earth space environment and the mesosphere is the coldest region in the ~~earth's~~-Earth's atmosphere. Polar Mesosphere Summer Echoes (PMSE) are strong echoes detected by radars from medium frequency (MF) to ultra-high frequency (UHF) bands in polar summer mesopause, and PMSE has been considered to be possible indicators of global climate change (Thomas and Olivero, 2001). ~~On average, the strongest echo occurs at the altitude of about 86 km, and the~~The observation range is from 75- to 100 km where on average, the strongest echo occurs at the altitude of about 86 km (Czechowsky et al., 1979). Radar waves in the very high frequency (VHF) band are backscattered ~~by~~due to irregularities of ~~the~~electron density with spatial scales of about half the radar wavelength: This was confirmed by Blix et al. (2003) from simultaneous rocket and radar observations. ~~(Blix et al., 2003). These polar mesospheric summer echoes (PMSE) are fundamentally related to the ice particles in mesospheric ice clouds (Rapp and Lübken, 2004). Even though this theory has been presented incompletely, it still provides a great impetus for the research of PMSE generation mechanism. The most extensively accepted theory is that the irregularities of electron density is sustained due to the reduction in electron diffusion characterized by the slowest ambipolar diffusion mode associated with the charged ice grains (Cho et al., 1992). The most extensively accepted theory is that the electron diffusion was characterized by the slowest ambipolar diffusion mode associated with the charged ice grains (Cho et al., 1992).~~Varney et al. (2011) scrutinized one particular aspect of the turbulent theory of PMSE: the electron density dependence of the echo strength. One remarkable feature of all PMSE is the fact that the radar echoes often occur in the form of two or more distinct layers that can persist for periods of up to several hours. Until now, the layering mechanism leading to these multiple structures is only poorly understood in spite of some previous attempts involving gravity waves, the general thermal structure, and Kelvin-Helmholtz-instabilities (Röttger, 1994; Klostermeyer, 1997; Hill et al., 1999; Hoffmann et al., 2005).

Palmer et al. (1996) statistically analyzed the PMSE in northern hemisphere observed by the EISCAT VHF radar during 1988-1993. ~~Palmer et al. (1996) presented a statistical study of PMSE, after analyzed the observations of the EISCAT VHF radar during 1988-1993. They suggested that~~confirmed that: (1) PMSE are summer phenomena, lasting from June to August; ~~these echoes are a summer phenomenon in the Northern hemisphere, lasting from June to August;~~ (2) PMSE occur mostly around noon and midnight, following a semidiurnal pattern; (3) the echoing structures move bodily, perhaps in response to gravity

设置了格式: 字体颜色: 着色 1

设置了格式: 字体颜色: 红色

waves. ~~based~~ Based on measurements at 53.5 MHz in at Andenes, Norway, ~~observed by the~~ with the 53.5 MHz ALOMAR SOUSY radar during 1994-1997 and ~~with~~ the ALWIN radar during 1999-2001. Bremer et al. (2003) ~~derived~~ found that the variation of PMSE is markedly controlled by solar cycle variations and precipitating high energetic particle fluxes. Bremer et al. (2006) discussed that the strength of PMSE depends on the level of ionization because of the long-term changes of mesospheric summer echoes caused by the incident solar wave radiation and precipitating high energetic particle fluxes from about 20 May to the end of August during 1998-2006. Smirnova et al. (2010) used the ESRAD MST radar's measurements; Yi et al. (2017) and found that the inter-annual variations of PMSE OR (occurrence ratio) and length of the season anticorrelated with solar activity represented by the ($F_{10.7}$ index, the daily solar activity proxy solar 10.7 cm radio flux) but not significant, and correlate with geomagnetic activity represented by (AP index) based on ESRAD MST radar measurements in Kiruna, Sweden. Nevertheless, no statistically significant trends in PMSE yearly strength occurrence ratio or in the length of the PMSE season were found in their paperwork. Smirnova et al. (2011) concentrated on the accurate calculation of PMSE absolute strength as expressed by radar volume reflectivity and found that the inter-annual variations of PMSE volume reflectivity strongly correlate with the local geomagnetic K-index and anticorrelate with solar 10.7 cm flux. but However, they did not find any statistically significant trend in PMSE volume reflectivity during 1997-2009. Li and Rapp (2011) reported that the correlations of the occurrence ratio of PMSE OR at 224 MHz shows a positive correlation with the both the solar and geomagnetic activities both show positive correlations. PMSE have been detected and widely studied based on long-term observations of many different MST radars (Reid et al., 2013 1989; Thomas et al., 1992; Smirnova et al., 2011) (Reid et al. 1989; Thomas et al. 1992; and Smirnova et al. 2011). since Since from the first observation of PMSE in 1979, it is well-known that the PMSE observations results are different when PMSE are observed by different frequency radar even at the same sites, and PMSEs often show obvious layered events.

Many studies have widely reported that there is significant correlation between the ionization level and PMSE observed by 53.5 MHz radar (Inhester et al., 1990; Belova et al., 2007; Latteck et al., 2008). Previous study by 53.5 MHz radar has provided the basic characteristics, the short term statistical variations of PMSE and the relation among the PMSE, solar activity and geomagnetic activity detected. The correlation of the ionization level with PMSE at 224 MHz, to the ionization level, however, is

设置了格式: 下标

设置了格式: 字体颜色: 着色 1

as significant as that, ~~the correlation of the ionization level with PMSE at 53.5 MHz to the ionization level, then previous studies~~ provides the research basis and ideas for the ~~research-PMSE study, detected by~~ 224MHz radar. There are still a few significant problems that must be solved with the characteristics of layered PMSE OR. Hence, it is necessary to analyze the ~~layered PMSE layered-OR~~ and study layered PMSE characteristics deeply with data measured by 224 MHz EISCAT VHF radar under different observation conditions. The statistical results of ~~layered PMSE layered-OR~~ with the same radar at the same site over the period 2004-2015 are given in this paper, which was based on the experiment data detected by 224 MHz EISCAT VHF radar. In addition, the ~~correlationrelationships~~ of PMSE OR with geomagnetic K index and $F_{10.7}$ ~~are~~ analyzed and discussed. The ~~PMSE OR calculation method of the correlation analysis between layered PMSE OR and solar activity and between layered PMSE OR and geomagnetic activity given in this paper without being affected by~~ solves the defect of discontinuous PMSE measurements that the measurements of EISCAT radar is discontinuous, which makes a significant breakthrough in the ~~calculation and~~ characterization of the ~~layered PMSE layered-OR, detected by EISCAT radar and~~ The aim of the current work is to provide the results could provide definitive data foundation for further analysis and the investigation of the physical mechanism of PMSE.

2 radar and experiment data description

The ~~experiment data of PMSE observations used here were~~ was obtained by with 224MHz EISCAT VHF radar from 2004 to 2015. EISCAT VHF The radar is located at Tromsø, Norway (69.35°N, 19.14°E), used ~~and a parabolic cylindrical 120m x 46m 40m antenna, with beam widths of 1.8° north south and 0.6° east west.~~ It is powerful tool for studying the lower ionosphere. Detailed descriptions of the radar can be found in Baron (1986). The measurements by EISCAT radar are very well suited for investigating the characteristics of PMSE. (for previous work, see e.g. Li et al., 2010 and references therein). It has frequency and phase modulation capability with pulse length of 1 μ s to 2 ms . Furthermore, reliable information of the raw electron density about PMSE, which is not derived by analysis of the incoherent scatter spectrum, but power profiles or near zero lag data can be obtained by EISCAT radar. The level of electron density represents the intensity of echoes. The parameters described are shown in Table 1 for accuracy control of EISCAT VHF radar.

设置了格式: 字体颜色: 着色 1

设置了格式: 下标

EISCAT VHF radar ran several standard experiment modes: “manda, beata, bella, tau7, arcd (arc_dlayer) and tau1”. The main differences between ~~the arcd and manda~~ these experiment modes are illustrated in Table 2. The manda and arcd modes mainly used for low altitude detection, and provide spectral measurements at mesospheric altitude. Therefore, the accurate data used in this study is mainly given provided by manda and arcd modes. ~~The Grand Unified Incoherent Scatter Design and Analysis Program (GUIDAP) software package have been used for analyzing the EISCAT VHF radar data. The electron density N_e analyzed by GUIDAP software was obtained between 10^6 and 10^{14} m^{-3} .~~

. Table 1 Parameters of the radars.

Radar	EISCAT VHF
Location	69.59° N 19.23° E
Operating frequency	224 MHz
Transmitter peak power	1.5 MW
Antenna 3-dB beam width	1.7° NS \times 1.2° EW
Antenna effective area	5690 m ²
Pulse length (altitude resolution)	300 m
Pulse repetition frequency	741 Hz
No. of bits in code	64
No. of code permutations	128
No. of coherent integrations	1
Lag resolution	1.35 ms
Maximum lag	0.17 s

Table 2 EISCAT VHF radar standard experiments.

Name	Code length [bit]	Baud length [μs]	Sampling rate [μs]	Range span [km]	Time resolution [s]	Plasma line	Raw data
manda	61	2.4	1.2	19–209	4.8	-	Yes
arc_dlayer	64	2	2	60–139	5.0	-	-
beata	32	20	20	52–663	5.0	Yes	-
bella	30	45	45	63–1344	3.6	Yes	-
tau7	16	96	12	50–2001	5.0	-	-
tau1	16	72	24	104–2061	5.0	-	-

带格式表格

3 Data analysis

In this study we have used the EISCAT VHF radar data from 2004 to 2015. The software package GUISDAP (Grand Unified Incoherent Scatter Design and Analysis Program) (see Lehtinen and Huuskonen, 1996 and www.eiscat.se for details) was used for analyzing radar data. The electron density N_e analyzed by GUISDAP software was obtained between 10^6 and 10^{14} m^{-3} . The level of electron density represents the intensity of echoes.

First of all, the heating parts were removed from the data set to avoid the heating effect. After that, the presence of PMSE was defined as the threshold of electron density ($N_e > 2.6 \times 10^{11}$ m^{-3}). We used the PMSE threshold given by Hocking and Röttger (1997) and Qiang Li (2011b) (see Appendix A Table A.2). Besides, some abnormal echoes are related to the meteor are not considered to be PMSE and is neglected in later discussion. PMSE is not continuous in time, so if the electron density satisfies the threshold ($N_e > 2.6 \times 10^{11}$ m^{-3}), we considered it as a PMSE event. We have considered only those events for which PMSE echoes are continuous for time ($t \geq 1$ min).

4 Results

4.1 Layered PMSE Occurrence ratios events

PMSE occur in thin layers having thickness up to 3-4 km, and the mean altitude distribution of PMSE events is 80-90km. It is considered to be the area of independent abnormal-anomalous echoes. Fig. 1 (a), (b) and(c) show the typical events of PMSE monolayer, double-layer and tri-layer, respectively. As mentioned in the introduction, a notable feature of PMSE observed by radar is that radar echoes typically occur in the form of two or more layers. However, the system theories of the layering mechanism led to these multiple structures didn't come into being. One remarkable feature of all PMSE is the fact that the radar echoes often occur in the form of two or more distinct layers that can persist for periods of up to several hours. Until now, the layering mechanism leading to these multiple structures is not well understood. Here we are will studying the occurrence of these layered PMSE multiple-layer events and

带格式的: 正文, 缩进: 左侧: 0.19 厘米, 行距: 2 倍行距

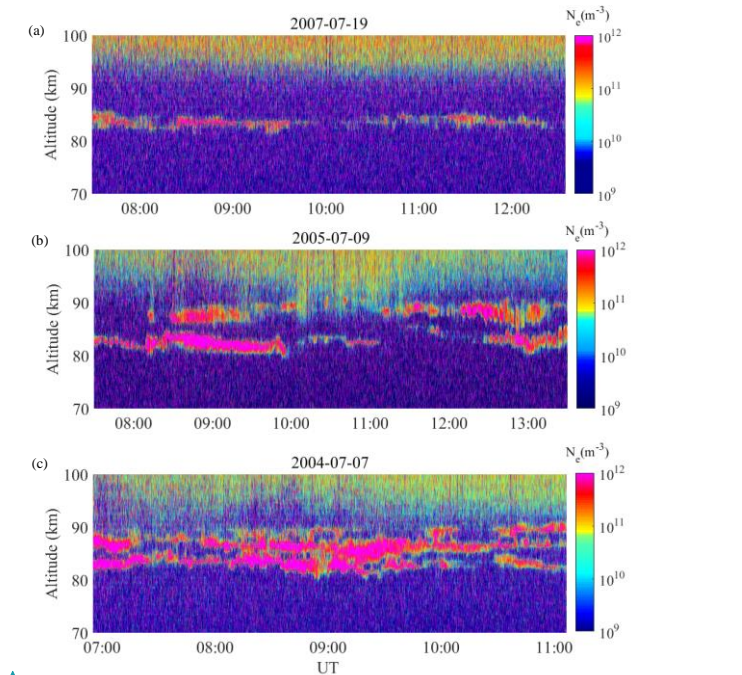
设置了格式: 字体: (默认) 等线, (中文) 等线

设置了格式: 字体: (中文) Times New Roman, 字距调整三号

带格式的: 标题 1, 行距: 单倍行距

带格式的: 标题 2, 缩进: 左侧: 0.19 厘米

its relationship with solar and geomagnetic activity. This content will be discussed in detail later in the [article paper](#).



5 **Fig. 1** The typical layered PMSE events observed by EISCAT 224MHz VHF radar. **a)** The observation on 19 July, 2007 (Upper panel) Monolayer PMSE; **b)** The observation on 9 July, 2005 (Middle panel) Double layer PMSE; **c)** The observation on 7 July, 2004 (lower panel) Tri-layer PMSE. The red circle marks the obvious layered phenomenon of PMSE events.

10 **3.4.1.2 Layered PMSE OR Calculation-calculation method**

The calculation method is based on individual horizontal profiles. When the electron density satisfies the PMSE threshold ($N_e > 2.6 \times 10^{11} \text{ m}^{-3}$), then that time was taken as the starting time of the PMSE occurrence and until the time when the electron density fails to satisfy the threshold was taken as the end time of PMSE occurrence. The time of PMSE duration is the time difference between the end and the starting time of the PMSE occurrence. The time interval not be regarded as PMSE occurrence time, if the time interval between them is shorter than 1 minute ($t < 1 \text{ min}$). Taking the calculation method of

域代码已更改

带格式的: 两端对齐

设置了格式: 非上标/下标

monolayer PMSE OR as an example: We defined that the ratio between the sustained time of monolayer PMSE and the total observation time as the monolayer PMSE OR. The applied procedure for the detection of multiple PMSE layers is based on individual vertical profiles with a high temporal resolution (Hoffmann, 2004). The layer ranges are identified by an electron density threshold of $2.6 \times 10^{11} \text{ m}^{-3}$ ($N_e > 2.6 \times 10^{11} \text{ m}^{-3}$). Once a vertical profile of the electron density has two peaks and these two peaks are higher than the threshold ($N_e > 2.6 \times 10^{11} \text{ m}^{-3}$), we select it as a double layer. The PMSE double-layer OR is the ratio between the sustained time of PMSE double layer and the total observation time. The tri-layer OR is also calculated by using the same way.

设置了格式: 字体: 倾斜

设置了格式: 字体: 倾斜, 下标

设置了格式: 字体: 倾斜

设置了格式: 字体: 倾斜, 下标

To find the characteristic of PMSE occurrence ratio (OR), a computing method and threshold must be defined. First of all, the data during radar heating experiments has been eliminated. After that, the number of data points satisfying the threshold of electron density ($N_e > 2.6 \times 10^{11} \text{ m}^{-3}$) was calculated (Hocking and Röttger, 1997). PMSE is not continuous in time, so if the number of data points satisfying the electron density threshold of PMSE were less than 8 data points in any time interval, these data points were replaced with the average of electron density (N_e) of 80-90 km regardless of the threshold (Rauf et al., 2018). It maintained the original electron density values at the corresponding time, so that the correlation is not influenced. The correlation coefficients have been calculated between PMSE OR and the 10.7cm of the solar flux index (F10.7), PMSE OR and geomagnetic events K indices, respectively. Because we chose the integration time of manda and ared models are 4.8s and 2s respectively, on the basis of the condition ($t \geq 1 \text{ min}$), the PMSE is needed to be simultaneous for ≥ 12 and 30 data points, respectively. What's more, some abnormal echoes are related to the precipitation particle areas are not considered to be PMSE and is neglected in later discussion.

设置了格式: 字体: (中文) + 中文正文 (等线)

带格式的: 正文, 缩进: 左侧: 0.19 厘米

设置了格式: 字体颜色: 着色 6

设置了格式: 字体颜色: 紫色

设置了格式: 字体颜色: 着色 2

The emphasis of this paper is to present a hybrid algorithm based on grid partitioning. The calculation method is based on time. Taking the calculation method of PMSE monolayer occurrence ratio as an example, the all electron density detected by the EISCAT VHF radar are counted, and the electron density with the value larger than the threshold in this time period are taken out. The ratio between the sustained time of monolayer PMSE and the total observation time is obtained. At different heights, when an electron density value greater than the threshold and less than the threshold is continuously alternate observed in an observation region with altitude range from 3-4km, we consider that double layer or multi-

设置了格式: 字体颜色: 着色 2

设置了格式: 字体颜色: 着色 1

设置了格式: 字体颜色: 自动设置

设置了格式: 字体颜色: 着色 1

layer-PMSE events occur. The PMSE double-layer OR is the ratio between the sustained time of PMSE double layer and the total observation time. The tri-layer OR is also calculated in this way.

3.4.2.3 The variations of layered PMSE layered-occurrence ratios

For studying the The layered PMSE layered-OR, layered PMSE layered-occurrence time (OT) and total observing time detected by EISCAT VHF radar from 2004 to 2015 were are illustrated in Table 3. PMSE mono-, double-, tri-layer and total OR were are also presented in Table 3 as well.

Table 3 Statistical data from 2004 to 2015.

Year	Total Observing Time (#min)	Monolayer PMSE OT (min)/min	Double Layer PMSE OT (min)/min	Tri-ple layer PMSE OT (min)/min	Monolayer OR [%]	Double layer OR [%]	Triple-Tri-layer OR [%]	Total OR [%]
2004	16054	4701	2774	151	29.28%	17.28%	0.94%	47.50%
2005	8165	3564	1491	182	43.65%	18.26%	2.23%	64.14%
2006	9248	2950	910	93	31.78%	9.84%	1.01%	42.63%
2007	9341	3027	804	0	32.41%	8.61%	0.00%	41.02%
2008	3310	763	97	0	23.06%	2.92%	0.00%	25.98%
2009	2264	424	76	8	18.72%	3.34%	0.35%	22.41%
2010	6303	1799	498	53	28.54%	7.90%	0.84%	37.28%
2011	9638	3624	2692	202	37.60%	27.93%	2.10%	67.63%
2012	7497	3550	1554	207	47.35%	20.73%	2.76%	70.84%
2013	14037	6906	3873	532	49.20%	27.59%	3.79%	80.59%
2014	2971	998	731	64	33.60%	24.6%	2.15%	60.35%
2015	4776	2019	1022	22	42.28%	21.40%	0.46%	64.14%

带格式的: 居中
带格式的: 居中
带格式的: 居中
带格式的: 居中
带格式表格

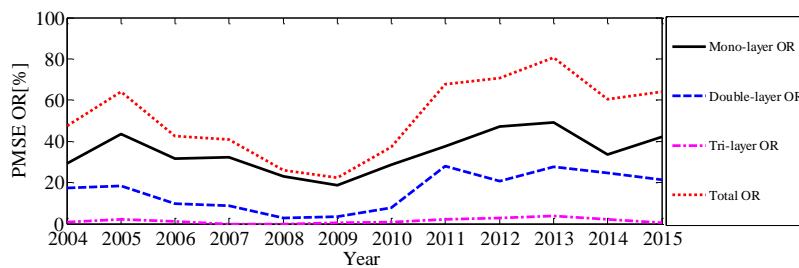


Fig. 2 Layered PMSE layered-occurrence ratio. The OR of total (red dot line). The OR of monolayer (black solid line). The OR of double-layer (blue dashed line). The OR of triple-layer (pink dot-dashed line).

Fig. 2 shows that the mono- double- and triple-layer OR agrees with the total PMSE OR. We calculated the correlation of mono-layer with double-layer OR, tri-layer OR and total OR using the Spearman rank correlation coefficients (It will be particular described in section 4.3.2).-between mono-layer OR and double-layer OR, mono-layer OR and tri layer OR, mono layer OR and Total OR, respectively. The correlation coefficients (r_s) of mono-layer with double-layer OR, tri-layer OR and total OR are 0.7922, 0.7718 and 1, respectively. All the correlation coefficients are statistically significant with reached very significant level($P<0.05$), respectively. These high values of correlation coefficients show that the correlation of mono-layer with double-layer OR, tri-layer OR, and total OR is very high. -In addition, the layered PMSE layered-OR from 2008 to 2010 is relatively low, and the solar activity was-is relative 'quiet' in these years.

Fig. 2 shows Two-two significant phenomena-can be discovered from Fig-2: One was (1) theThe variation trends of layered-mono-, double- and tri-layer PMSE OR of PMSE-is-is rules to follow different but regular-. That is i.e., the OR of monolayer is the highest, double-layer lies in the middle and the triple-layer is the lowest-. The other(2) was-The layered PMSE layered-and total OR values show similar shape of sinusoidal, which has obvious wave peak and wave valley. One wave peak lies in the year about 2005 and; the other lies in the year 2013. The values of two wave peaks are different; and the values in 2005 are smaller than that in 2013. The values of wave valley lie in 2008-2009. Meanwhile, the gap between two peaks of PMSE OR is about 7 or 8 years. Here we only give the results of the data analysis, no longer do the cause analysis, because the stratification of PMSE is affected by many factors and has yet to be decided. The analyzing method and the results drawn during the process of given in this paper have a significant certain reference value for right and in depth researching studying the PMSE phenomenon.

34.3.4 Seasonal behaviour

The mean seasonal variations of the layered PMSE layered-OR and PMSE total OR observed by EISCAT VHF radar during 2004-2015 were is shown in Fig. 3 and Fig. 4, respectively. Fig. 3 illustrates the mean seasonal variation of the mono- (blue bars) double- (yellow bars) and tri-layer (red bars) PMSE OR and quarticsecond order polynomial fitting for the monolayer PMSE OR (black dot-curve) during 2004-2015.

Fig. 4 shows the mean seasonal variation of PMSE total OR (blue bars) and $3/\pi$ harmonic fitting second order polynomial fit for total PMSE OR (black dot-curve) during 2004-2015. It can beis derived clear

设置了格式: 字体颜色: 着色 1

设置了格式: 字体颜色: 自动设置

设置了格式: 字体颜色: 自动设置

设置了格式: 字体颜色: 绿色

设置了格式: 字体颜色: 红色

from Fig. 3 and Fig. 4 that the monolayer PMSE events in the Tromsø, Norway, often begins in late May, reaches its maximum in early June or mid-June, keeps this level until the end of July or beginning of August, and gradually decreases or vanishes when it is close to the end of August or the beginning of September in general, which ~~wai~~ is in agreement with ~~references~~(Smirnova et al., (2011)). The double-layer PMSE also begins in late May, but its maximum appears in mid-July. In addition, it keeps the larger value in June and July, and simply fade away in early August. The ~~triple~~-layer PMSE appears a lot less in comparison to mono- ~~and~~, double- layer PMSE. In terms of time, it appears later and disappears earlier. ~~What's Further~~more, the ~~triple-tri~~- layer PMSE OR is large in end of June and early July, which is different than monolayer and double layer PMSE OR.

10 According to the statistical results, ~~PMSE~~-monolayer, double-layer and ~~multilayer-tri-layer~~ PMSE OR have seasonal variation. ~~Moreover, there is fluctuation in the trends of $F_{10.7}$ and geomagnetic K-indices. In addition, the trends of F10.7 and geomagnetic K index also fluctuates.~~ Therefore, it is necessary to investigate the correlation of solar and geomagnetic activity ~~on~~-with different layered PMSE OR during 2004-2015, and ~~better~~-try to explain the ~~occurrence~~ mechanism of PMSE. It is well known that other missions apart from PMSE regular observations are performed by EISCAT VHF radar, so EISCAT radar does not provide continuous PMSE observations. ~~Just by noting that there have a few deviations by methods of calculating layered PMSE OR, we~~We raise an important question: Table 3 indicates a difference in total observation time for the individual years. How has this been taken into account for the determination of occurrence ratios? ~~To solve this problem~~Therefore, we use another method to recalculate the ~~layered~~ PMSE ~~layered~~-OR. Then the correlation between the ~~layered~~ PMSE ~~layered~~-OR and the $F_{10.7}$ and between the ~~layered~~ PMSE ~~layered~~-OR and K index ~~were are~~ studied. As mentioned in the calculation method section, we only select the days ~~when where~~ PMSE is ~~existed~~present and calculate the layered ~~occurrence ratio~~OR of PMSE.

设置了格式: 下标

设置了格式: 下标

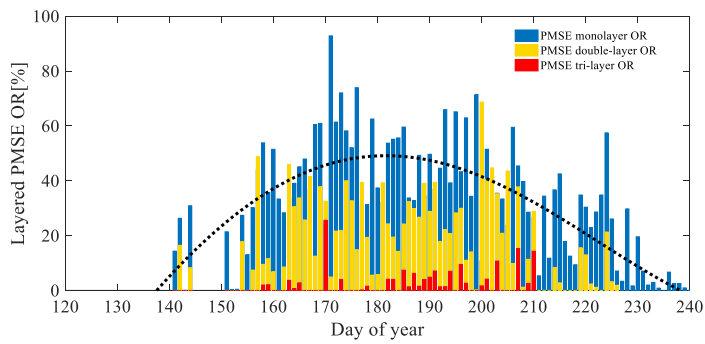
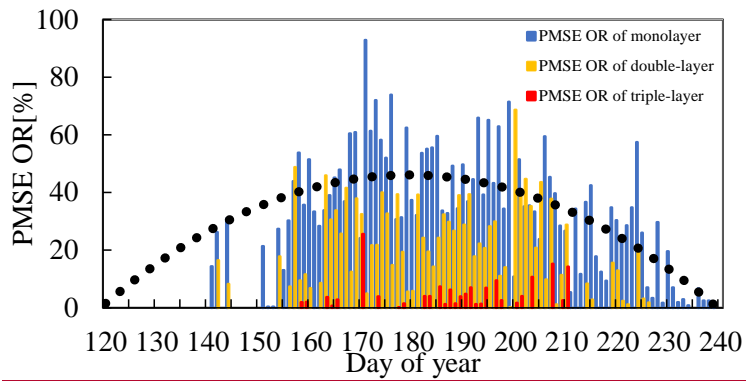


Fig. 3 Mean seasonal variation of the PMSE mono-(in blue), double-(in yellow), triple-layer (in red) PMSE occurrence ratio at Tromsø using observations from 2004 to 2015.

带格式的: 行距: 单倍行距

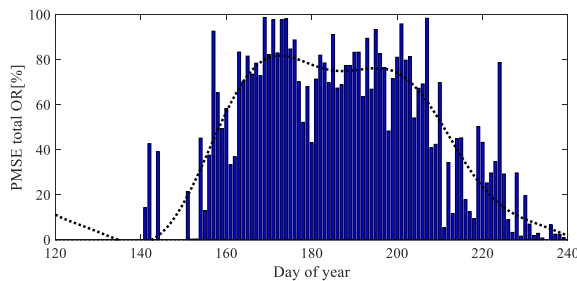
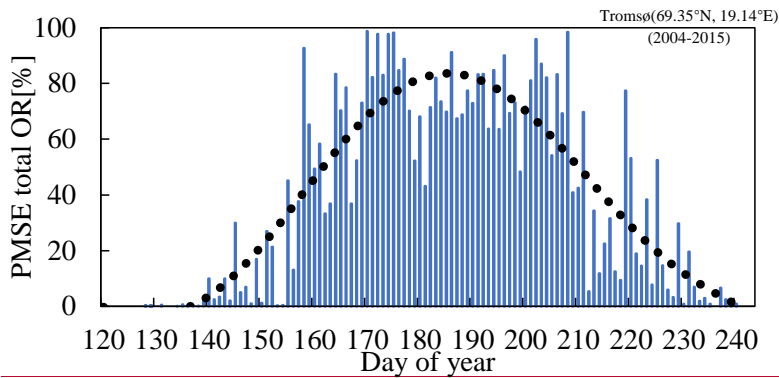


Fig. 4 Mean seasonal variation of the PMSE total PMSE occurrence ratio.

4.5 Discussion

5 We have calculated the layered PMSE layered OR was calculated and the relations among PMSE
 mono-, double- and triple- layer OR were analyzed statistically. At the same time, the mean seasonal
 variations of the layered PMSE OR and PMSE total OR have been presented. Hoffmann
 (2004) shows that the layering occurs because of subsequent nucleation cycles of ice particles in the
 uppermost (and coldest) gravity wave induced temperature minimum (see Hoffmann, 2004, Figure 3a).
 10 Subsequently, these newly created ice particles grow and sediment down and lead to the distinct layering.
 Besides, it is now generally accepted that both Rapp and Lübken (2004) found that charged ice particles
 and atmospheric turbulence play major roles in the change of the electron number density that leads to
 PMSE in the mesopause region (Rapp and Lübken, 2004). We know that solar and geomagnetic activities
 have a certain degree of influence on the occurrence of PMSE, but however, the effects of solar and
 15 geomagnetic activities on layered PMSE are not clear understood well. Therefore, it is necessary to study

the effects of solar and geomagnetic activities on layered PMSE. The occurrence ratio obtained by the ratio of the occurrence time of PMSE to the total observation time is the calculation method in the traditional sense. It is easy to understand and accurately analyze the short-term variations, such as diurnal variation and seasonal variation of PMSE. However, the long-term trend is **subject to error and dispute** inaccurate by using this calculation method, **because the radar measurement data is not continuous.** ~~And Furthermore,~~ it is difficult to discuss and analyze the **correlation of layered PMSE OR with solar relations between PMSE and solar activities and between PMSE and geomagnetic activities.** Therefore, we have ~~designed~~ **presented** a new calculation method for calculating the **layered PMSE layered** occurrence ratio, which is **based on the height** different from the method given in section 4.2. So that, the **layered occurrence of PMSE becomes continuous,** and the long-term variations of **PMSE OR is becomes** easy and relatively accurate. **The correlation of PMSE with solar and geomagnetic activities is not expected to affect by discontinuous PMSE.** The study of relations between PMSE and solar activities and between PMSE and geomagnetic activities ~~can be studied~~ **are** significant.

45.1 Another method for layered PMSE OR ~~Calculation~~ Calculation method

The calculation method is based on altitude. A large number of literatures and experimental observations have shown that the altitude range of PMSE is 80-90km (Li and Rapp, 2011; Smirnova et al., 2010; Latteck and Bremer, 2013). Among all the altitude and electron density observed by EISCAT VHF radar, we only take the apparent electron density in the altitude range of 80-90km, and then take out the electron density greater than the threshold in the period when the PMSE is known to be present. The ratio between the numbers of layered PMSE electron densities values greater than the threshold and the numbers of total electron density in the range of 80-90 km was calculated respectively. The double-layer and tri-layer PMSE OR obtained by this method have a higher occurrence ratio than the first method.

The emphasis of this section is to present a hybrid algorithm based on grid partitioning. The calculation method is based on altitude. A large number of literatures and experimental observations have shown that the altitude range of PMSE is 80-90km (Li and Rapp, 2011; Smirnova et al., 2010; Latteck and Bremer, 2013). Hoffmann (2004) shows a mean height of 84.8 km for monolayer PMSE, whereas in the case of multiple layers PMSE, the lower layer occurs at a mean height of ~83.4 km. For the second layer

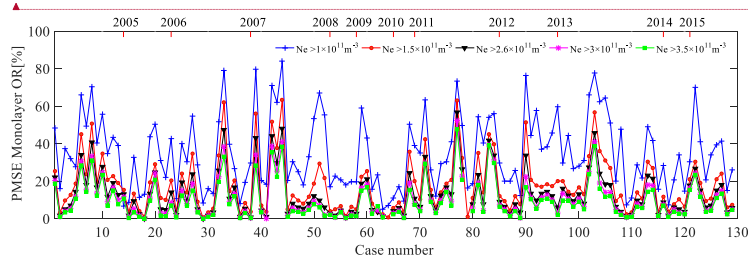
带格式的: 标题 2, 缩进: 左侧: 0.19 厘米

带格式的: 缩进: 左侧: 0.09 厘米

in the case of multiple PMSE layer structures shows a maximum at about 86.3 km (The judging criteria in regard to the multiple layer PMSE see section 4.3). Firstly, we counted the total number of electron density at altitude of 80-90km and then counted the number of electron density satisfying the PMSE threshold ($N_e > 2.6 \times 10^{11} \text{m}^{-3}$) in the period when the PMSE is known to be present (if electron density satisfies the threshold $N_e > 2.6 \times 10^{11} \text{m}^{-3}$, we identify layered PMSE exist at this moment). The ratio between the numbers of layered PMSE electron densities values larger than threshold and the numbers of total electron density at altitude of 80-90 km was calculated. The double-layer and tri-layer PMSE OR calculated by this method is higher than the layered PMSE OR calculated by the method given in section 4.2. The correlation coefficients were calculated between PMSE OR and the 10.7cm of the solar flux index ($F_{10.7}$) and between PMSE OR and geomagnetic K index, respectively. The PMSE have been identified only for the time of PMSE duration lager than 1 min ($t \geq 1$ min). Because the integration time of manda and arcd models are 4.8s and 2s respectively, on the basis of the condition ($t \geq 1$ min), the PMSE is needed to be for ≥ 12 and 30 data points, respectively.

设置了格式: 下标

45.2 Layered PMSE-layered OR under different electron density threshold



设置了格式: 字体: (中文) + 中文正文 (等线), 英语(英国)

Fig. 5 PMSE monolayer occurrence ratio under different electron density threshold conditions with axis at top showing the time in years. Vertical lines are the end of 2006 and 2011, respectively (black dashed line). The legends on the figure is the average of PMSE occurrence rate in three time periods separated by the black dashed line.

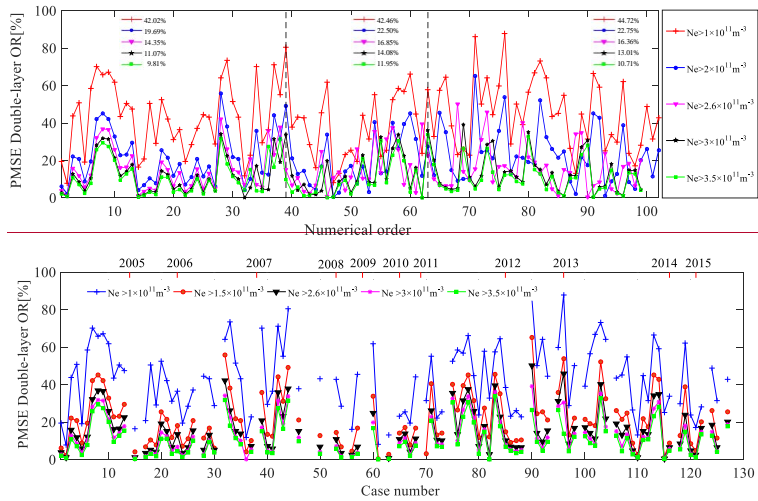


Fig. 6 PMSE double-layer occurrence ratio under different electron density threshold conditions with axis at top showing the time in years. Vertical lines are the end of 2006 and 2011 (black dashed line). The legends on the figure is the average of PMSE occurrence rate in three time periods separated by the black dashed line.

5

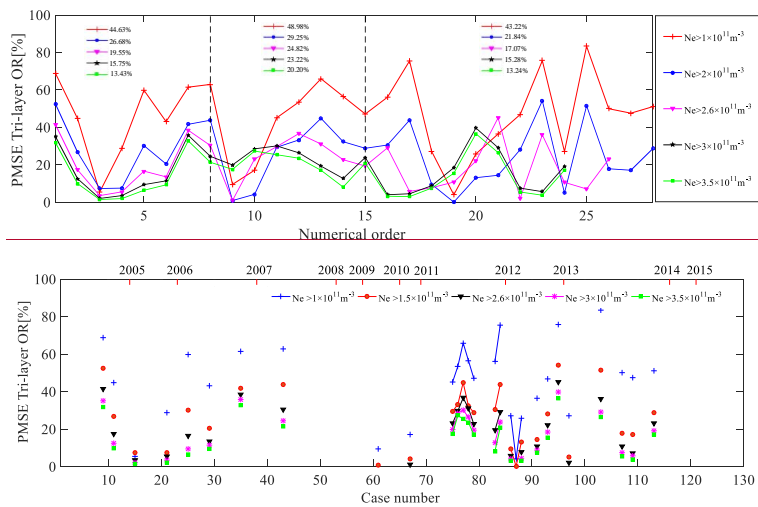


Fig.7 PMSE tri-layer occurrence ratio under different electron density threshold conditions with axis at top showing the time in years. Vertical lines are the end of 2006 and 2011 (black dashed line). The legends on the figure is the average of PMSE occurrence rate in three time periods separated by the black dashed line.

10

In this section, the day when the first occurrence of PMSE in 2004 (regardless of duration) was recorded as 1, and the day with the later occurrence of PMSE increased by sequence. Using this sequence as the horizontal axis and the layered PMSE layered-OR with different electron density threshold as the vertical axis, the results are shown in Fig. 5, 6, and 7. That is, Fig. 5, Fig. 6 and Fig. 7 show PMSE mono- double- and tri-layer OR under different electron density threshold-conditions, respectively. In the calculation method section we said that we have defined the electron density threshold ($N_e >> 2.6 \times 10^{11} \text{m}^{-3}$). Here, we give the layered PMSE layered-OR with threshold conditions of $N_e >> 1 \times 10^{11} \text{m}^{-3}$, $N_e >> 1.5 \times 10^{11} \text{m}^{-3}$, $N_e >> 2.6 \times 10^{11} \text{m}^{-3}$, $N_e >> 3 \times 10^{11} \text{m}^{-3}$ and $N_e >> 3.5 \times 10^{11} \text{m}^{-3}$, respectively. We can get their found the variation trends of layered PMSE OR with different threshold to be are largely consistent, in addition, the larger the threshold, the smaller the ratio. Smirnova et al. (2010) analyzed day-to-day and year-to-year variations of PMSE OR for different thresholds. They found that the choice of the threshold does not influence the shape of the variation curves for PMSE OR. Zeller and Bremer (2009) indicated that different threshold values are for the investigations of the influence of geomagnetic activity on PMSE, however, of less importance. They both think that the variation trends of PMSE OR with different threshold are consistent. The aim of choosing 5 different thresholds is also to increase the number of samples for calculating the correlation coefficients between layered PMSE OR and F10.7 and between layered PMSE OR and K index. Since these occurrence ratios are calculated in the case where the occurrence of PMSE is determined, there is no case of missing data, and it can be recognized that these occurrence rates are reliable. The legends on the figure is the average of PMSE mono-, double- and triple-layer OR with threshold conditions of $N_e > 1 \times 10^{11} \text{m}^{-3}$, $N_e > 1.5 \times 10^{11} \text{m}^{-3}$, $N_e > 2.6 \times 10^{11} \text{m}^{-3}$, $N_e > 3 \times 10^{11} \text{m}^{-3}$ and $N_e > 3.5 \times 10^{11} \text{m}^{-3}$ during the periods of 2004-2006, 2007-2011 and 2012-2015. It is well known that the period of 2006-2009 is solar minimum and 2012 is solar maximum, but the PMSE mono- and double-layer average OR in 2007 is not consistent with solar activity. In other words, there has is no obvious correlation between PMSE mono- and double-layer PMSE OR and solar activity. What's more, we found that PMSE triple-layer OR and solar activity in opposite directions. To prove the conclusion, we will calculate the correlation coefficient between layered PMSE layered-OR and solar activity and between layered PMSE layered-OR and geomagnetic activity in next section. Therefore, the correlation relation between them can be judged directly.

设置了格式: 字体: (默认) Times New Roman, 10 磅

设置了格式: 字体: (默认) Times New Roman, 10 磅, 字体颜色: 红色

设置了格式: 字体: (默认) Times New Roman, 10 磅, 字体颜色: 红色

设置了格式: 非突出显示

设置了格式: 字体: (默认) Times New Roman, 10 磅, 字体颜色: 红色

设置了格式: 字体: (默认) Times New Roman, 10 磅, 字体颜色: 红色

设置了格式: 字体颜色: 着色 6

设置了格式: 字体颜色: 自动设置

设置了格式: 字体颜色: 自动设置

设置了格式: 字体颜色: 自动设置, 非突出显示

设置了格式: 字体颜色: 自动设置

45.3 Effect of solar and geomagnetic activity on PMSE OR

45.3.1 $F_{10.7}$ index and K -index

The $F_{10.7}$ index is a measure of the solar radio flux per unit frequency at a wavelength of 10.7 cm, near the peak of the observed solar radio emission. $F_{10.7}$ is often expressed in SFU or solar flux units (1 SFU = 10^{-22} W·m⁻²·Hz⁻¹). It represents a measure of diffuse, nonradiative coronal plasma heating. It is an excellent indicator of overall solar activity levels and correlates well with solar UV emissions. The K-index quantifies disturbances in the horizontal component of ~~earth's~~ Earth's magnetic field with an integer in the range 0-9 with 1 being calm and 5 or more indicating a geomagnetic storm. It is derived from the maximum fluctuations of horizontal components observed on a magnetometer during a three-hour interval. The K-index was introduced by Julius Bartels in ~~1938~~ 1939 (Bartels et al., 1939). The K index values used in the paper is the median of the K index observed on a magnetometer during a day, ~~which where has removed~~ the effects of the heating experiments ~~were removed~~.

45.3.2 Correlation coefficients

A correlation coefficient is a numerical measure of some type of correlation, meaning a statistical relationship between two variables (Boddy and Smith, 2009). The Pearson correlation coefficient known as Pearson's r , is a measure of the strength and direction of the linear relationship between two variables that is defined as the covariance of the variables divided by the product of their standard deviations. ~~This is the best known and most commonly used type of correlation coefficient.~~ Pearson's correlation coefficient Given a pair of random variables (X, Y), the formula for r is (Wilks, 1995):

$$r_{X,Y} = \frac{\text{cov}(X,Y)}{\sigma_X \sigma_Y}$$

Where:

Cov is the covariance.

σ_X is the standard deviation of X

σ_Y is the standard deviation of Y .

Spearman's rank correlation coefficient is a measure of how well the relationship between two variables can be described by a monotonic function. The Spearman correlation between two variables is equal to the Pearson correlation between the rank values of those two variables. While Pearson's correlation assesses linear relationships, Spearman's correlation assesses monotonic relationships (whether linear or

设置了格式: 下标

设置了格式: 下标

设置了格式: 下标

not) (Well and Myers, 2003). For a sample of size n , the n raw scores X_i, Y_i are converted to ranks rgX_i, rgY_i , and r_s is computed from:

$$r_s = \frac{\text{cov}(rgX, rgY)}{\sigma_{rgX} \sigma_{rgY}}$$

Where:

5 $\text{cov}(rgX, rgY)$ is the covariance of the rank variables.

σ_{rgX} and σ_{rgY} are the standard deviations of the rank variables.

A high value (approaching +1.00) is a strong direct relationship, values near 0.50 are considered moderate and values below 0.30 are considered to show weak relationship. A low negative value (approaching -1.00) is similarly a strong inverse relationship, and values near 0.00 indicate little, if any
10 relationship.

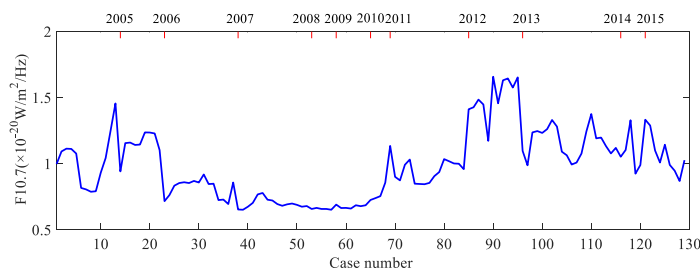
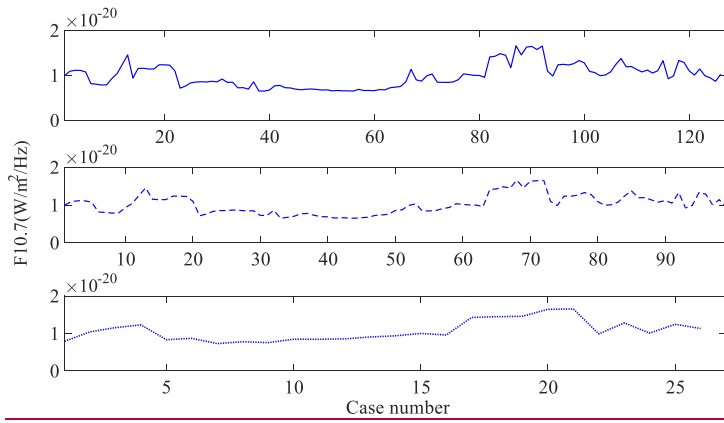
To determine whether a result is statistically significant, a P -value is calculated, which is the probability of observing an effect of the same magnitude or more extreme given that the null hypothesis is true (Devore, 2011). The null hypothesis is rejected if the P -value is less than a predetermined level (usually $\alpha=0.05$). Where α is called the significance level, and is the probability of rejecting the null
15 hypothesis given that it is true (a type I error).

带格式的: 缩进: 首行缩进: 1 字符

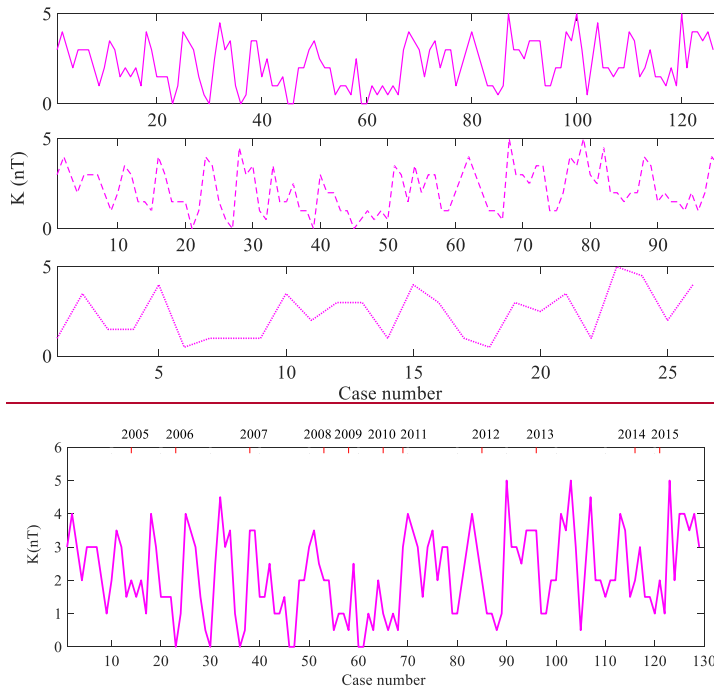
设置了格式: 字体: 倾斜

45.3.3 Correlation between layered PMSE OR, $F_{10.7}$ and K index

设置了格式: 下标



(a)



(b)

Fig. 8 (a) The variations of $F_{10.7}$ values corresponding to the occurrence of PMSE with axis at top showing the time in years. Upper panel: $F_{10.7}$ values corresponding to the occurrence of mono-layer PMSE; Middle panel: $F_{10.7}$ values corresponding to the occurrence of double-layer PMSE; lower panel: $F_{10.7}$ values corresponding to the occurrence of triple-layer PMSE. (b) The variations of geomagnetic K index values corresponding to the occurrence of PMSE with axis at top showing the time in years. Upper panel: K index values corresponding to the occurrence of mono-layer PMSE; Middle panel: K index values corresponding to the occurrence of double-layer PMSE; lower panel: K index values corresponding to the occurrence of triple-layer PMSE.

设置了格式: 下标

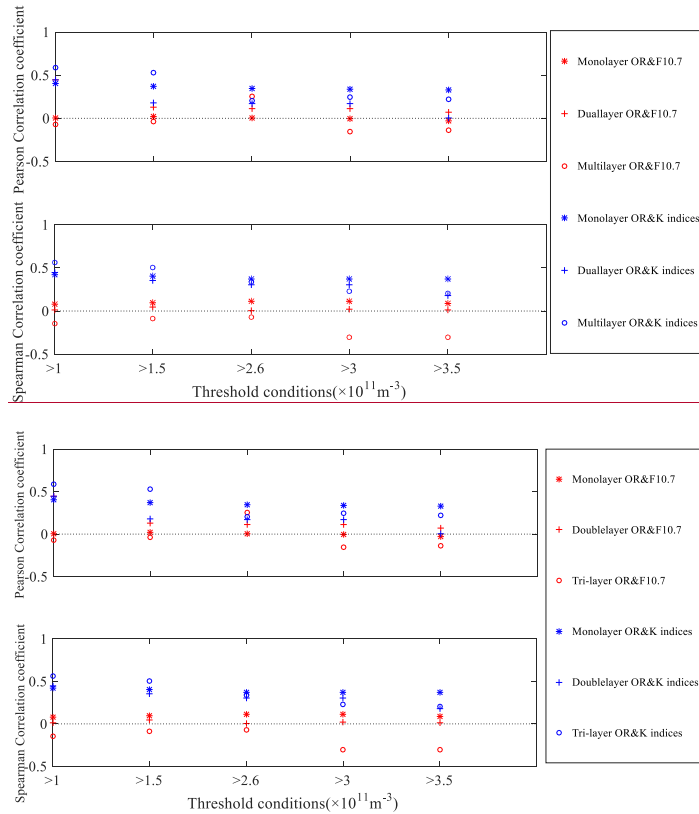


Fig. 9 Pearson linear and Spearman rank correlation computed between layered PMSE OR (with thresholds conditions of $N_e \gg 1 \times 10^{11} \text{m}^{-3}$, $N_e \gg 1.5 \times 10^{11} \text{m}^{-3}$, $N_e \gg 2.6 \times 10^{11} \text{m}^{-3}$, $N_e \gg 3 \times 10^{11} \text{m}^{-3}$ and $N_e \gg 3.5 \times 10^{11} \text{m}^{-3}$, respectively) and $F_{10.7}$ corresponding to the occurrence of PMSE and between layered PMSE OR and K index corresponding to the occurrence of PMSE, respectively. For each correlation coefficient, P value is less than 0.05. The horizontal dotted line is drawn to separate positive and negative correlation coefficients.

Fig.8 shows that the variations of $F_{10.7}$ and geomagnetic K index values corresponding to the occurrence of PMSE. The correlation of PMSE with solar and geomagnetic activities is not expected to affect by discontinuous PMSE, Since the $F_{10.7}$ and K values corresponding to the occurrence of PMSE with threshold of $N_e > 2.6 \times 10^{11} \text{m}^{-3}$. The $F_{10.7}$ and K values corresponding to the occurrence of PMSE with threshold conditions of $N_e > 2.6 \times 10^{11} \text{m}^{-3}$. So, the study of relations between PMSE and solar activities and between PMSE and geomagnetic activities make sense. Combined-The relation between layered PMSE OR and $F_{10.7}$ and between layered PMSE OR and K values can be analyzed for the results shown in conjunction with Figures 5 through 8. with Fig. 5, 6, and 7, we can roughly analyze the relationship

设置了格式: 下标

设置了格式: 字体: 倾斜

设置了格式: 下标

带格式的: 缩进: 左 0.5 字符

设置了格式: 下标

设置了格式: 字体: (默认) Times New Roman, 10 磅

设置了格式: 下标

between the layered PMSE OR and the F10.7 and between the layered PMSE OR and K values, but the results may be relatively inaccurate.

In order to ~~examine~~ study the correlation between layered PMSE OR and $F_{10.7}$ and between layered PMSE OR and K index, all the data points of PMSE OR, $F_{10.7}$ and K index with simultaneous occurrence were combined.

Fig.9 shows the correlation coefficients computed by combing all the points of PMSE OR (with thresholds-conditions of $N_e \gg 1 \times 10^{11} m^{-3}$, $N_e \gg 1.5 \times 10^{11} m^{-3}$, $N_e \gg 2.6 \times 10^{11} m^{-3}$, $N_e \gg 3 \times 10^{11} m^{-3}$ and $N_e \gg 3.5 \times 10^{11} m^{-3}$), $F_{10.7}$ and K index with simultaneous occurrence and apply significant test.

It ~~can be~~ seen from Fig.9 that layered PMSE OR is positively correlated with the K index and the coefficients indicate moderate correlation between the variables, but Whereas the correlation coefficient between PMSE mono- and $F_{10.7}$, double-layer OR

and $F_{10.7}$ both are very low, indicating that their correlation is weak or even not relevant. Interestingly, we found that the PMSE tri-layer OR has a negative correlation with $F_{10.7}$, although the correlation was lower than what we have supposed, this finding has never published in previous any existing literature.

Hence, it is indicated that the cases with positive values play a decisive role when calculating the correlation coefficient between the data points of PMSE and K index occur simultaneously, and events with negative values dominate in the calculation of the correlation coefficient between PMSE

tri-layer PMSE OR and $F_{10.7}$. But PMSE mono-, double- layer PMSE OR has hardly relevance with $F_{10.7}$.

The correlation between layered PMSE layered-OR and $F_{10.7}$ and between layered PMSE layered-OR and K index were have been obtained.

It indicates that there are many complicated factors for the formation and development of PMSE besides the solar and geomagnetic activities. There are explanations for these results: on one hand, the enhanced solar activity increases the electron density due to the increase of ionization, and with the increase of solar radiation, the photodissociation enhance and the water vapor content is reduced.

On the other hand, the positive correlation between PMSE OR and K index may be apprehensible as because of the enhanced magnetic activity caused precipitating particles increase in the mesosphere, and lead to increase in electron densities.

Latteck and Bremer (2013) shows that PMSE are caused by inhomogeneities in the electron density of the radar Bragg scale within the plasma of the cold summer mesopause region in the presence of negatively charged ice particles. Thus, the occurrence of PMSE contains information about mesospheric temperature and water vapor content but also depends on the ionization due to solar electromagnetic radiation and precipitating high energetic particles.

But

设置了格式: 下标
设置了格式: 下标

设置了格式: 下标

设置了格式: 下标

设置了格式: 下标

设置了格式: 下标

设置了格式: 字体颜色: 着色 1

设置了格式: 下标

设置了格式: 下标

设置了格式: 字体: (中文) 宋体

设置了格式: 下标

设置了格式: 字体颜色: 红色

However, ~~still we still can't can not~~ explain why there is a negative correlation between tri-layer PMSE OR and $F_{10.7}$. ~~This should be focused in future or this may be our future research focus.~~

设置了格式: 下标

5-6 Summary and Conclusions

带格式的: 缩进: 左 0.5 字符, 行距: 固定值 17 磅

In the paper, ~~we presented the~~ PMSE occurrence ratios with monolayer, double- and ~~triple-~~layers ~~that were detected by EISCAT VHF radar during a solar cycle have been presented. It was obtained that the~~ The daily ~~variation~~ and seasonal variation of the layered PMSE ~~was analysed.~~ We implemented a ~~new~~ method to provide more accurate conclusions on the study of the long-term variation of PMSE with different thresholds. ~~Then the~~ The correlation ~~relationship~~ between layered PMSE and solar radiation flux ($F_{10.7}$) and between layered PMSE and geomagnetic activity (K index) ~~were was~~ given. The following

设置了格式: 下标

conclusions were reached:

- (1) Mono-, double- and tri-layer PMSE have different seasonal behavior. Monolayer PMSE events often begins in late May, reaches its maximum in early June or mid-June, keeps this level until the end of July or beginning of August, and gradually decreases or vanishes when it is close to the end of August or the beginning of September in general, which ~~was is~~ in agreement with ~~earlier report~~ ~~references~~ (Smirnova et al., 2011). The double-layer PMSE OR reaches ~~maximum in mid-July~~ ~~its maximum appears in mid-July~~ and simply fade away in early August. The ~~triple-~~layer PMSE appears later and disappears earlier in comparison to mono- ~~and~~ double-layer PMSE, and it is large in end of June and early July.
- (2) The variation trends of ~~PMSE~~ mono- double- and tri-layer PMSE OR under different electron density thresholds ~~conditions are largely greatly~~ consistent. It is ~~found was got~~ that the larger the threshold, the smaller the ratio. Beyond that, PMSE mono- and double-layer OR ~~were are~~ not associated with solar activity. and PMSE ~~triple-~~layer OR is inversely proportional to solar activity.
- (3) Layered PMSE ~~layered~~ OR is positively correlated with the K index. The correlation between PMSE mono- and double-layer OR and $F_{10.7}$ is relatively weak, and PMSE tri-layer OR has a negative correlation with $F_{10.7}$.

设置了格式: 下标

设置了格式: 下标

Data availability:

All EISCAT data used in this work have been downloaded at <https://www.eiscat.se/schedule/schedule.cgi>.

Competing interests. The authors declare that they have no conflict of interest.

Authors' contributions

Shucan Ge designed this study, carried out statistics, analyzed the results and wrote the manuscript.

5 Hailong Li participated in the design of the study and the analysis of the results. Tong Xu and Mengyan Zhu helped with the conceptual ideas for the paper. Maoyan Wang and Lin Meng managed this study and participated in language grammar modification. Safi Ullah and Abdur Rauf participated in modifying language issues and provided a lot of suggestions about revised manuscript. All authors read and approved the final manuscript.

10 **Acknowledgments**

This study is supported by the National Natural Science Foundation of China [No. 41104097 and No.41304119]. This study is also supported by the National Key Laboratory of Electromagnetic Environment, China Research Institute of Radiowave Propagation (CRIRP). We also acknowledge EISCAT, which is an international association supported by China, Finland, Japan, Norway, Sweden, and
15 the UK. *I would like to thank Wen Yi who has contributed to this revised manuscript.*

References

Bartels, J., Heck, N. A. H., and Johnston, H. F.: The Three-Hour-Range Index Measuring Magnetic Activity, *Journal of Geophysical Research*, 44, 411-454, doi.org/10.1029/TE044i004p00411, 1939.

20 Baron, M.: EISCAT progress 1983-1985. *Journal of Atmospheric and Terrestrial Physics*, 48, 767-772, doi: 10.1016/0021-9169(86)90050-4, 1986.

Belova, E., P. Dalin, and Kirkwood, S.: Polar mesosphere summer echoes: A comparison of simultaneous observations at three wavelengths, *Annales Geophysicae*, 25, 2487-2496, doi: 10.5194/angeo-25-2487-2007, 2007

25 Blix, T. A., Rapp, M., and Lübken, F. J.: Relations between small scale electron number density fluctuations, radar backscatter, and charged aerosol particles, *Journal of Geophysical Research Atmospheres*, 108, 1-10, doi:org/10.1029/2002JD002430, 2003.

Boddy, R., and Smith, G.: *Statistical Methods in Practice: for Scientists and Technologists*, John Wiley & Sons Ltd Chichester, 2009.

30 Bremer, J., Hoffmann, P., Latteck, R., and Singer, W.: Seasonal and long-term variations of PMSE from VHF radar observations at Andenes, Norway, *Journal of Geophysical Research Atmospheres*, 108, doi:org/10.1029/2002JD002369, 2003.

设置了格式: 字体颜色: 自动设置, 字距调整三号

带格式的: 标题 1, 行距: 单倍行距

设置了格式: 字距调整三号

带格式的: 缩进: 左侧: 0 厘米, 悬挂缩进: 2 字符, 首行缩进: -2 字符, 行距: 单倍行距

带格式的: 缩进: 左侧: 0 厘米, 悬挂缩进: 2 字符, 首行缩进: -2 字符, 行距: 单倍行距

- Bremer, J., Hoffmann, P., Höffner, J., Latteck, R., Singer, W., Zecha, M., and Zeller, O.: Long-term changes of mesospheric summer echoes at polar and middle latitudes, *Journal of Atmospheric and Solar-Terrestrial Physics*, 68, 1940-1951, doi:org/10.1016/j.jastp.2006.02.012, 2006.
- Cho, J. Y. N., Hall, T. M., and Kelley, M. C.: On the Role of Charged Aerosols in Polar Mesosphere Summer Echoes, *Journal of Geophysical Research Atmospheres*, 97, 875-886, doi:org/10.1029/91JD02836, 1992.
- Czechowsky, P., Rueter, R., and Schmidt, G.: Variations of mesospheric structures in different seasons, *Geophysical Research Letters*, 6, 459-462, doi:org/10.1029/GL006i006p00459, 1979.
- Devore, J. L.: *Probability and Statistics for Engineering and the Sciences (8th ed.)*. Boston, MA: Cengage Learning, 300-344. ISBN 978-0-538-73352-6, 2011.
- Hill, R. J., D. E. Gibson-Wilde, J. A. Werne and D. C. Fritts: Turbulence-induced fluctuations in ionization and application to PMSE, *Earth Planets Space*, 51, 499-513, doi: 10.1186/BF03353211, 1999.
- Hocking, W. K., and Röttger, J.: Studies of polar mesosphere summer echoes over EISCAT using calibrated signal strengths and statistical parameters, *Radio Science*, 32, 1425-1444, doi:org/10.1029/97RS00716, 1997.
- Hoffmann, P.: On the occurrence and formation of multiple layers of polar mesosphere summer echoes. *Geophysical Research Letters*, 32 (5), L05812, doi: 10.1029/2004gl021409, 2005.
- Inhester, B., Ulwick, J., Cho, J., Kelley, M. and Schmidt, G.: Consistency of rocket and radar electron density observations: implications about the anisotropy of turbulence, *Journal of Atmospheric and Solar-Terrestrial Physics*, 52, 855-873, doi: 10.1016/0021-9169(90)90021-e, 1990.
- Klostermeyer, J.: A height- and time-dependent model of polar mesosphere summer echoes. *Journal of Geophysical Research: Atmospheres*, 102(D6), doi: 10.1029/96JD03652, 1997.
- Latteck, R., Singer, W., Morris, R. J., Hocking, W. K., Murphy, D. J., Holdsworth, D. A. and Swarnalingam, N.: Similarities and differences in polar mesosphere summer echoes observed in the Arctic and Antarctica, *Annales Geophysicae*, 26, 2795-2806, doi: 10.5194/angeo-26-2795-2008, 2008
- Latteck, R., and Bremer, J.: Long-term changes of polar mesosphere summer echoes at 69°N, *Journal of Geophysical Research Atmospheres*, 118, 10441-10448, doi:10.1002/jgrd.50787, 2013.
- Lehtinen, M.S., Huuskonen, A.: General incoherent scatter analysis and GUIDSAP, *Journal of Atmospheric and Solar-Terrestrial Physics*, 58, 435-452, doi: 10.1016/0021-9169(95)00047-x, 1996.
- Li, Q., Rapp, M., Röttger, J., Latteck, R., et al.: Microphysical parameters of mesospheric ice clouds derived from calibrated observations of polar mesosphere summer echoes at Bragg wavelengths of 2.8 m and 30 cm, *Journal of Geophysical Research*, 115, D00I13, doi:10.1029/2009JD012271, 2010.
- Li, Q., and Rapp, M.: PMSE-observations with the EISCAT VHF and UHF-radars: Statistical properties, *Journal of Atmospheric and Solar-Terrestrial Physics*, 73, 944-956, doi:org/10.1016/j.jastp.2010.05.015, 2011.
- Palmer, J. R., Rishbeth, H., Jones, G. O. L., and Williams, P. J. S.: A statistical study of polar mesosphere summer echoes observed by EISCAT, *Journal of Atmospheric and Solar-Terrestrial Physics*, 58, 307-315, doi:org/10.1016/0021-9169(95)00038-0, 1996.
- Rapp, M., and Lübken, F. J.: Polar mesosphere summer echoes (PMSE): review of observations and current understanding, *Atmospheric Chemistry and Physics*, 4, 2601-2633, doi:org/10.5194/acp-4-2601-2004, 2004.

带格式的: 缩进: 左侧: 0 厘米, 悬挂缩进: 2 字符, 首行缩进: -2 字符, 行距: 单倍行距

带格式的: 缩进: 左侧: 0 厘米, 悬挂缩进: 2 字符, 首行缩进: -2 字符, 行距: 单倍行距

Rapp, M. and Lübken, F.-J.: Polar mesosphere summer echoes (PMSE): Review of observations and current understanding. *Atmospheric Chemistry and Physics*, 4(11/12), 2601-2633, doi:10.5194/acp-4-2601-2004, 2004.

设置了格式: 字体: (中文) 宋体, 字体颜色: 黑色

Rauf, A., Li, H., Ullah, S., Meng, L., Wang, B., and Wang, M.: Statistical study about the influence of particle precipitation on mesosphere summer echoes in polar latitudes during July 2013, *Earth Planets and Space*, 108(70), doi:org/10.1186/s40623-018-0885-6, 2018.

Reid, I. M., Czechowsky, P., Ruster, R., and Schmidt, G.: First VHF radar measurements of mesopause summer echoes at mid-latitudes, *Geophysical Research Letters*, 16, 135-138, doi:org/10.1029/GL016i002p00135, 1989.

设置了格式: 字体颜色: 着色 1

Röttger, J.: Middle atmosphere and lower thermosphere processes at high latitudes studied with the EISCAT radars. *Journal of Atmospheric and Solar-Terrestrial Physics*, 56(9):1173-1195, doi: 10.1016/0021-9169(94)90056-6, 1994.

带格式的: 缩进: 左侧: 0 厘米, 悬挂缩进: 2 字符, 首行缩进: -2 字符, 行距: 单倍行距

Smirnova, M., Belova, E., Kirkwood, S., and Mitchell, N.: Polar mesosphere summer echoes with ESRAD, Kiruna, Sweden: Variations and trends over 1997–2008, *Journal of Atmospheric and Solar-Terrestrial Physics*, 72, 435-447, doi:10.1016/j.jastp.2009.12.014, 2010.

设置了格式: 字体颜色: 着色 1

Smirnova, M., Belova, E., and Kirkwood, S.: Polar mesosphere summer echo strength in relation to solar variability and geomagnetic activity during 1997–2009, *Annales Geophysicae*, 29, 563-572, doi:10.5194/angeo-29-563-2011, 2011.

Thomas, L., Astin, I., Prichard, I. T.: The characteristics of VHF echoes from the summer mesopause region at mid-latitudes. *Journal of Atmospheric and Terrestrial Physics*, 54(7-8), 969-977, doi: 10.1016/0021-9169(92)90063-q, 1992.

带格式的: 缩进: 左侧: 0 厘米, 悬挂缩进: 2 字符, 首行缩进: -2 字符, 行距: 单倍行距

Thomas, G. E., and Olivero, J.: Noctilucent clouds as possible indicators of global change in the mesosphere, *Advances in Space Research*, 28, 937-946, 2001.

Varney, R. H., Kelley, M. C., Nicolls, M. J., Heinselman, C. J., and Collins, R. L.: The electron density dependence of polar mesospheric summer echoes, *Journal of Atmospheric and Solar-Terrestrial Physics*, 73, 2153-2165, doi:org/10.1016/j.jastp.2010.07.020, 2011.

Well, A. D., and Myers, J. L.: *Research design and statistical analysis*, New York, 1-736, 2003.

Wilks, D. S.: *Statistical Methods in the Atmospheric Sciences*, Burlington, MA: Academic Press, 1995.

Yi, W., Reid, I. M., Xue, X., Younger, J. P., Murphy, D. J., Chen, T., and Dou, X.: Response of neutral mesospheric density to geomagnetic forcing, *Geophysical Research Letters*, 44, 8647-8655, doi:org/10.1002/2017GL074813, 2017.

Zeller O. and Bremer J., The influence of geomagnetic activity on mesospheric summer echoes in middle and polar latitudes, *Annales Geophysicae*, 27(2): 831-8372, DOI: 10.5194/angeo-27-831-2009, 2009.